The FEBS Journal

FEBS PRESS science publishing by scientists

Analysis of proximal *ALOX5* promoter binding proteins by quantitative proteomics

Katharina Schlag, Dieter Steinhilber, Michael Karas and Bernd L. Sorg

Institute of Pharmaceutical Chemistry/ZAFES, Goethe-University, Frankfurt am Main, Germany

Keywords
5-lipoxygenase; DNA G-quadruplex; DNA pulldown; DNA-protein-interactions; label-free quantitative mass spectrometry

Correspondence
B. L. Sorg, Institute of Pharmaceutical Chemistry/ZAFES, Goethe-University, 60438 Frankfurt am Main, Germany
Tel: +49-69-798-29337
E-mail: b.sorg@pharmchem.uni-frankfurt.de
and
M. Karas, Institute of Pharmaceutical Chemistry/ZAFES, Goethe-University, 60438 Frankfurt am Main, Germany
Tel: +49-69-798-29916
E-mail: karas@pharmchem.uni-frankfurt.de

(Received 5 June 2019, revised 15 October 2019, accepted 23 February 2020)

doi:10.1111/febs.15259

5-Lipoxygenase (5-LO) is the initial enzyme in the biosynthesis of leukotrienes, which are mediators involved in pathophysiological conditions such as asthma and certain cancer types. Knowledge of proteins involved in 5-LO pathway regulation, including gene regulatory proteins, is needed to evaluate all options for therapeutic intervention in these diseases. Here, we present a mass spectrometric screening of *ALOX5* promoter-interacting proteins, obtained by DNA pulldown and label-free quantitative mass spectrometry. Protein preparations from myeloid and B-lymphocytic cell lines were screened for promoter DNA interactors. Through statistical analysis, 66 proteins were identified as specific *ALOX5* promotor binding proteins. Among those, the 15 most likely candidates for a prominent role in *ALOX5* gene regulation are the known *ALOX5* interactors Sp1 and Sp3, the related factor Sp2, two Krüppel-like factors (KLF13 and KLF16) and six other zinc finger proteins (MAZ, PRDM10, VEZF1, ZBTB7A, ZNF281 and ZNF579). Intriguingly, we also identified two helicases (BLM and DHX36) and the proteins hnRNPD and hnRNPK, which are, together with the protein MAZ, known to interact with DNA G-quadruplex structures. As G-quadruplexes are implicated in gene regulation, spectroscopic and antibody-based methods were used to confirm their presence within the GC-rich sequence of the *ALOX5* promoter. In summary, we have systematically characterized the interactome of the *ALOX5* promoter, identifying several zinc finger proteins as novel potential *ALOX5* gene regulators. Further, we have shown that the *ALOX5* promoter can form DNA G-quadruplex structures, which may play a functional role in *ALOX5* gene regulation.

Introduction

5-Lipoxygenase (5-LO) is the central enzyme in the leukotriene pathway of arachidonic metabolism [1]. Leukotrienes are potent lipid mediators that play a role in the pathogenesis of several inflammatory diseases, such as asthma, rheumatoid arthritis and inflammatory bowel disease [2]. Furthermore, the enzyme is implicated in the pathogenesis of certain forms of cancer and dysregulation of 5-LO gene expression has been observed in some tumour phenotypes [3–5]. This pathogenic involvement makes the regulation of 5-LO, including its gene regulation, an attractive target for therapeutic intervention [1,6,7].

Expression of human 5-LO occurs in a controlled, tissue-specific manner and is most prominently found in leucocytes. Among the myeloid cells, the enzyme is expressed in monocytes/macrophages, granulocytes, dendritic cells and mast cells. In the lymphoid lineage, 5-LO is found in B-lymphocytes, but not in T cells,

Abbreviations
1,25(OH_2) D_3, calcitriol (1α,25-dihydroxyvitamin D_3; 5-LO, 5-lipoxygenase; HRP, horseradish peroxidase; MM6, Mono Mac 6; TGFβ, transforming growth factor beta; TMB, 3,3′,5,5′-Tetramethylbenzidine; TMPyP4, Meso-5,10,15,20-Tetrakis-(N-methyl-4-pyridyl)porphine.

except for freshly isolated T cells [8,9]. Further, the enzyme is present in some brain regions [10].

In monocytic cells, prominent expression of 5-LO can be induced by the prodifferentiating agents transforming growth factor beta (TGFβ) and calcitriol (1α,25-dihydroxyvitamin D_3) [11,12]. In contrast, B-lymphocytes express 5-LO in a constitutive manner and are, in this respect, not TGFβ/calcitriol-responsive [13,14]. Mechanistically, TGFβ-responsiveness of *ALOX5* gene expression has been attributed – at least in part – to transcription initiation via SMAD binding elements in the proximal promoter and seems to involve MLL protein complexes [15,16]. Additionally, it could be demonstrated that calcitriol activates *ALOX5* transcript elongation and maturation [17,18]. A further mechanism of cell type-specific *ALOX5* regulation is promoter DNA methylation, leading to gene silencing in specific cell types [19].

The *ALOX5* core promoter region is GC-rich and lacks TATA or CAAT boxes. It contains eight GC boxes, five of which are arranged in tandem [20]. These GC boxes are functional binding sites for the transcription factors Sp1 and Egr-1 and are considered to be essential for basal transcriptional activity [8,21]. Naturally occurring mutations consist of the deletion of one or two Sp1-binding sites, or the addition of one Sp1-binding site to the (normally) five tandem GC boxes [22]. Although the functional consequences of these mutations are still unclear, a pharmacogenetic association between the mutant genotypes and responses to a 5-LO inhibitor (ABT-761) has been observed in a clinical trial for asthma [23]. Furthermore, several putative transcription factor binding sites have been predicted for the wider promoter-proximal region, among them NF-κB and AP-2 consensus sequences [20].

With regard to regulatory protein factors in *ALOX5* promoter regulation, most of the information available up to date originates from hypothesis-driven studies (reporter gene and gel shift assays), and an unbiased analysis is needed to appreciate all contributing factors. In this respect, MS-based quantitative proteomics provides a powerful tool for a screening of DNA–protein interactions. Formerly mainly used for the investigation of protein–protein interactions, affinity purification coupled to mass spectrometry likewise can be employed for elucidating DNA–protein interactions [24–28]. The recent establishment of MS methods and quantification strategies suitable for the analysis of dynamics and stoichiometries of protein–protein or protein–DNA complexes helped to improve their understanding [29–32]. Among these, label-free quantification provides a simple and fast protocol, without the need for additional labelling reactions. The analysis of differences in protein abundance in bait and control DNA pulldown and the enrichment of specific interactors can be carried out statistically, superseding further separation steps and allowing samples to be measured in a single LC-MS/MS run. Pulldown approaches provide sufficient sensitivity and selectivity for screening DNA sequences of interest [29] and identifying protein interactions, even if none of the binding partners is known. This helps to identify new potentially interacting transcription factors and recruited complex members for further functional studies.

In this study, we employed a workflow of DNA pulldowns coupled to label-free quantitative MS and statistical evaluation for the identification of novel promoter-interacting proteins. The promoter fragment used for pulldowns comprised positions −260 to −141 in relation to the translational start site (ATG) and contained the GC boxes that are considered the core promoter. To detect possible cell-specific binding patterns, we used the myeloid cell lines HL-60, THP-1 and Mono Mac 6 (MM6) (differentiated and undifferentiated), as well as B-lymphocytic cell lines Rec-1 and BL-41. We were able to confirm that Sp-family factors interact with the *ALOX5* promoter and introduce novel potential *ALOX5* gene regulators. Moreover, we identified a set of proteins as novel *ALOX5* promoter interactors associated with the recognition and binding of G-quadruplexes (also known as G4-DNA or G-tetraplexes) as secondary DNA structures. These are physiologically stable structures involved in the transcriptional control of certain genes that have attracted considerable interest due to their pharmacological relevance (reviewed in Ref. [33]). Accordingly, we analysed the used *ALOX5* promoter fragments and provide *in vitro* evidence for G-quadruplex formation thereof. Based on this, we suggest that G-quadruplex-based mechanisms may be involved in *ALOX5* gene regulation.

Results

DNA pulldowns: experimental set-up and validation

In our attempt to characterize the full range of *ALOX5* promoter-interacting proteins, we used a procedure which included the following five steps: (a) incubation of biotin-tagged *ALOX5* promoter DNA fragments, or corresponding control sequences, with nuclear extracts from 5-LO expressing cells; (b) binding of the protein-loaded DNA fragments to magnetic streptavidin beads; (c) magnetic separation of the

loaded beads and washing steps; (d) on-bead sample preparation for MS analysis by reduction, alkylation and enzymatic digestion; (e) protein identification by label-free quantitative MS and statistical evaluation. This workflow is depicted in Fig. 1.

The DNA fragments that served as bait in this pulldown assay were generated by annealing of complementary DNA oligonucleotides with a length of 120 nucleotides, of which the forward strands were 5′-biotin tagged (Fig. 2, Table S1, upper panel). The sequences of the DNA strands referred to as 'wild-type' (WT) correspond to position −260 to −141 of the *ALOX5* promoter region (in relation to the ATG) and thus encompass the GC boxes that are considered central to basal *ALOX5* promoter activity. The control fragment was designed by scrambling the WT sequences in order to maintain their relative base content, but eliminate existing consensus sequences for DNA-binding proteins (Table S1, lower panel). In order to verify correct hybridization to double-stranded fragments, the DNA was analysed by agarose gel electrophoresis before and after the annealing procedure (Fig. 3A).

As sources for the potential *ALOX5* promoter binding proteins, nuclear extracts were generated from three myeloid cell lines (HL-60, THP-1 and MM6) and from two B-cell lines (BL-41 and Rec-1). The three myeloid cell lines represent varying differentiation states of leucocytes: HL-60 cells are relatively immature and, depending on the treatment, can be differentiated towards granulocytes or monocytes [34]. THP-1 and MM6 cells, on the other hand, are already differentiated towards monocytes, with MM6 being more mature than THP-1 [35]. All three myeloid cell lines are known to upregulate 5-LO gene activity upon treatment with TGFβ/calcitriol [11,12,36]. In contrast, B-cell lines are known to express 5-LO constitutively [14]. We confirmed this expression pattern by western blotting (Fig. 3B).

In order to validate the basic functionality of the pulldown assay, we checked whether Sp1 as a known interactor of the *ALOX5* promoter could be specifically enriched from nuclear extracts. For this purpose, *ALOX5* promoter fragments served as the bait and scrambled (SCR) DNA sequences were used as a reference. The experiments were carried out with nuclear extracts from Rec-1 cells, which contain the ubiquitous transcription factor Sp1, and captured proteins were analysed by western blot using anti-Sp1 antibody. As depicted in Fig. 3C, pulldowns with the promoter fragment yielded about 4-(±1.5)-fold more Sp1 protein than those with SCR control DNA and therefore are suitable for specific enrichment and analysis of *ALOX5* promoter-interacting proteins.

MS detection of affinity-enriched proteins: Optimization of pulldown conditions and choice of quantification strategy

Next, we optimized the conditions of the pulldown assay with respect to MS identification of the enriched proteins. To this end, we performed titration experiments with varying amounts of both nuclear protein and DNA bait, as described by Hubner *et al.* [29]. Thus, WT *ALOX5* promoter DNA fragments in amounts of 10, 50, 100 and 250 pmol were incubated with 50, 100, 250 and 500 μg of nuclear protein from MM6 cells, respectively, and affinity-enriched proteins were analysed by MS. The number of identified peptides for four different proteins, which were reproducibly detected in initial pulldown experiments (Sp1, Sp3, KLF16 and MAZ) served as a measure of optimal conditions. From this trial, we found that 100 pmol of DNA bait in combination with at least 250 μg of nuclear protein is optimal for the identification of *ALOX5* promoter-interacting proteins (Fig. 4).

In a further optimization step, we compared MS quantification strategies that would allow for the identification of the maximum number of significant interactors from different DNA pulldown samples. Pulldown assays were performed with nuclear extracts from differentiated and undifferentiated HL-60 cells, and the number of proteins identified by dimethyl labelling-based quantification [37] was compared to the label-free method, respectively. In detail, HL-60 cells were either differentiated with 1 ng·mL^{-1} TGFβ and 50 nM calcitriol, or left untreated, for 3 days, and nuclear extracts were prepared. For each group, pulldowns were carried out using the WT *ALOX5* promoter fragment, or the SCR control as DNA bait. For the dimethyl labelling approach, peptide samples from WT and control groups were either labelled with light or heavy isotopes and combined afterwards. To avoid any bias that may be introduced by the labelling reaction itself, dimethyl labelling was carried out on cell duplicates with swatches of labels, as described in Boersema *et al.* [37]. Label-free experiments were carried out in triplicates for each differentiated and undifferentiated cells. Each duplicate or triplicate was subsequently subjected to statistical analysis to identify significant interactors. In total, 1244 proteins could be identified for undifferentiated cells in the dimethyl labelling approach compared to 1212 for label-free quantification (Fig. 5A). Except for a slight bias towards smaller molecular weights for the label-free

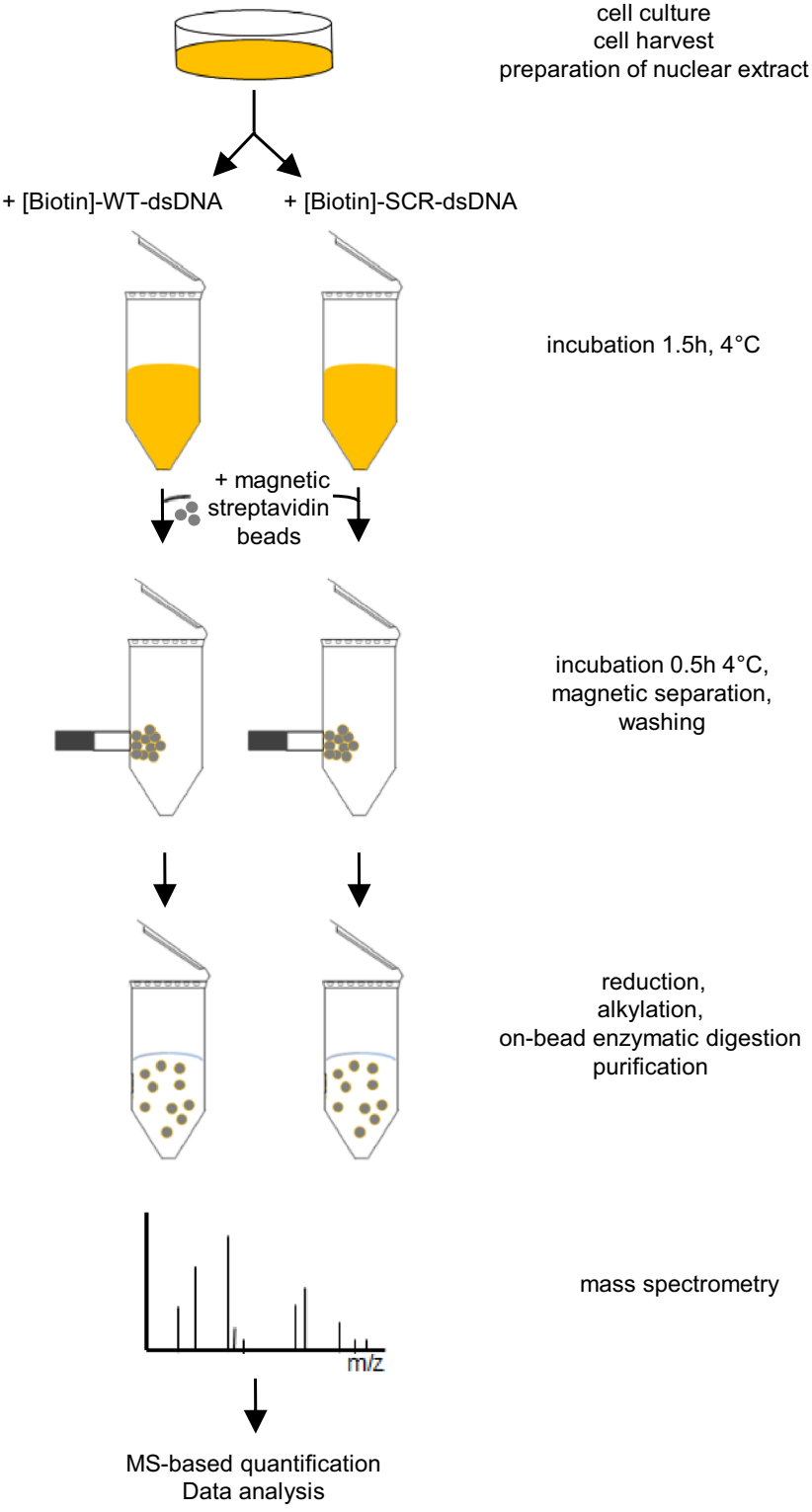

Fig. 1. Workflow for MS-based identification of *ALOX5* promoter-interacting proteins via DNA pulldown. Nuclear extracts were prepared from 5-LO expressing cells. Subsequently, biotin-tagged *ALOX5* promotor DNA fragments (WT) or corresponding control sequences (SCR) were incubated with the extracts. Protein-loaded DNA fragments were bound to magnetic streptavidin beads and separated magnetically. Finally, captured proteins were subjected to on-bead sample preparation steps and identified by MS.

approach, no major differences could be observed when comparing the physico-chemical properties of the identified proteins for both quantification strategies (Fig. 5B-D), pointing to the absence of bias for the different experimental set-ups. However, the higher overall identification of proteins for label-based

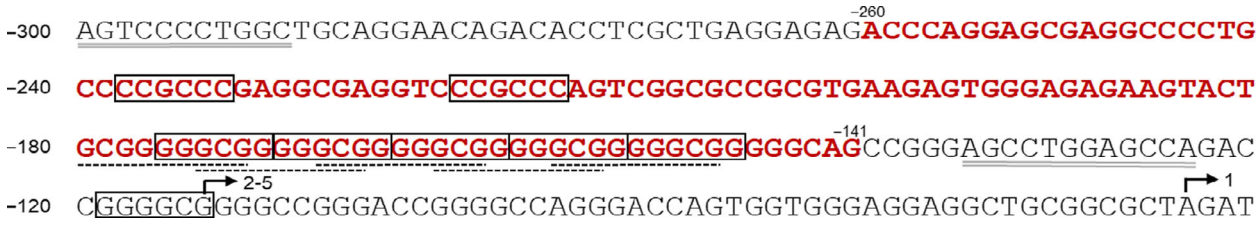

Fig. 2. Overview of the proximal *ALOX5* promoter sequence. Bases from pos. −61 to −300 of the human *ALOX5* gene are shown, with numbers relative to the translation start site. The sequence used in this study is given in boldface (in red). Transcription start sites for *ALOX5* mRNA isoforms 1 and 2–5 are indicated by arrows, flanked by the number of the corresponding isoform(s). Sp1 consensus sequences are boxed, Egr-1 consensus sequences are underlined with broken lines, and putative AP-2 binding sites are represented by double lines (in grey).

analysis did not contribute to a higher number of significant interactors, as a clearly higher number of significant interactors were identified by the label-free method for both differentiated and undifferentiated cells (Table 1).

Four out of five proteins identified as significantly interacting in undifferentiated, and six out of 13 in differentiated HL-60 for the dimethyl labelling approach were also present in the label-free pulldown. Thus, the overlap between the quantification strategies did not point to a fundamentally different output by either of the two methods. However, due to the higher number of significant interactors identified in this trial, label-free quantification was performed for all subsequent pulldowns.

Identification of ALOX5 promoter-interacting proteins from myeloid cell and B-cell lines

In order to identify *ALOX5* promoter-interacting proteins from the two most prominent 5-LO-positive cell lineages, we analysed samples from the myeloid cell lines HL-60, THP-1 and MM6 (both differentiated and undifferentiated), as well as from the two B cell lines BL-41 and Rec-1. For each cell type or condition, three independent experiments were carried out and enriched proteins were subjected to label-free MS analysis for protein identification. Statistical analysis was carried out from the triplicates, and the results were visualized in volcano plots (Fig. 6).

From the identified proteins, we focused on those that were detected in the MS analysis with at least one unique peptide, resulting in a list of 66 proteins (Table S2). Functional classification of the proteins in this dataset shows that the vast majority is involved in DNA/RNA turnover, with 24% of the proteins belonging to the family of transcription factors and 9% to transcriptional regulators (Fig. 7).

In order to further enhance the stringency of the results, this dataset was narrowed down to those proteins that (a) have been identified in at least two of the eight sample types (i.e. HL-60, THP-1, MM6, each differentiated/undifferentiated; Rec-1, BL-41) and (b) have a clear association to gene regulatory processes. These 15 proteins are listed in Table 2, and comprise 11 DNA-binding zinc finger transcription factors, two helicases and two hnRNP proteins.

The transcription factors include three Sp1 family proteins (Sp1, Sp2 and Sp3), two members of the related KLF family (KLF13 and KLF16), and six other zinc finger transcription factors (MAZ, PRDM10, VEZF1, ZBTB7A, ZNF281 and ZNF579). Of the latter six proteins, only MAZ, ZBTB7A and ZNF281 are fairly characterized. All of them bind to G/C-rich regulatory DNA elements and play a role in cell proliferation and differentiation and transcriptional regulation [38–43]. Interestingly, the protein MAZ has also been shown to bind to G-quadruplex structures and thereby to regulate gene expression. Among other genes, this has been observed for human *MYB* [44], which encodes the transcription factor Myb that is itself a known regulator of the *ALOX5* gene [45]. In line with the association of MAZ with G-quadruplex structures, the two helicases BLM and DHX36 [46,47] and the proteins hnRNPD and hnRNPK are also implicated with these DNA secondary structures [48,49], raising the question whether the *ALOX5* promoter sequence could harbour G-quadruplex structures.

In vitro G-quadruplex formation of the proximal ALOX5 promoter

To address the question whether G-quadruplex structures can form within the sequence context of the *ALOX5* promoter, we employed an established anti-DNA G-quadruplex antibody [50] and probed

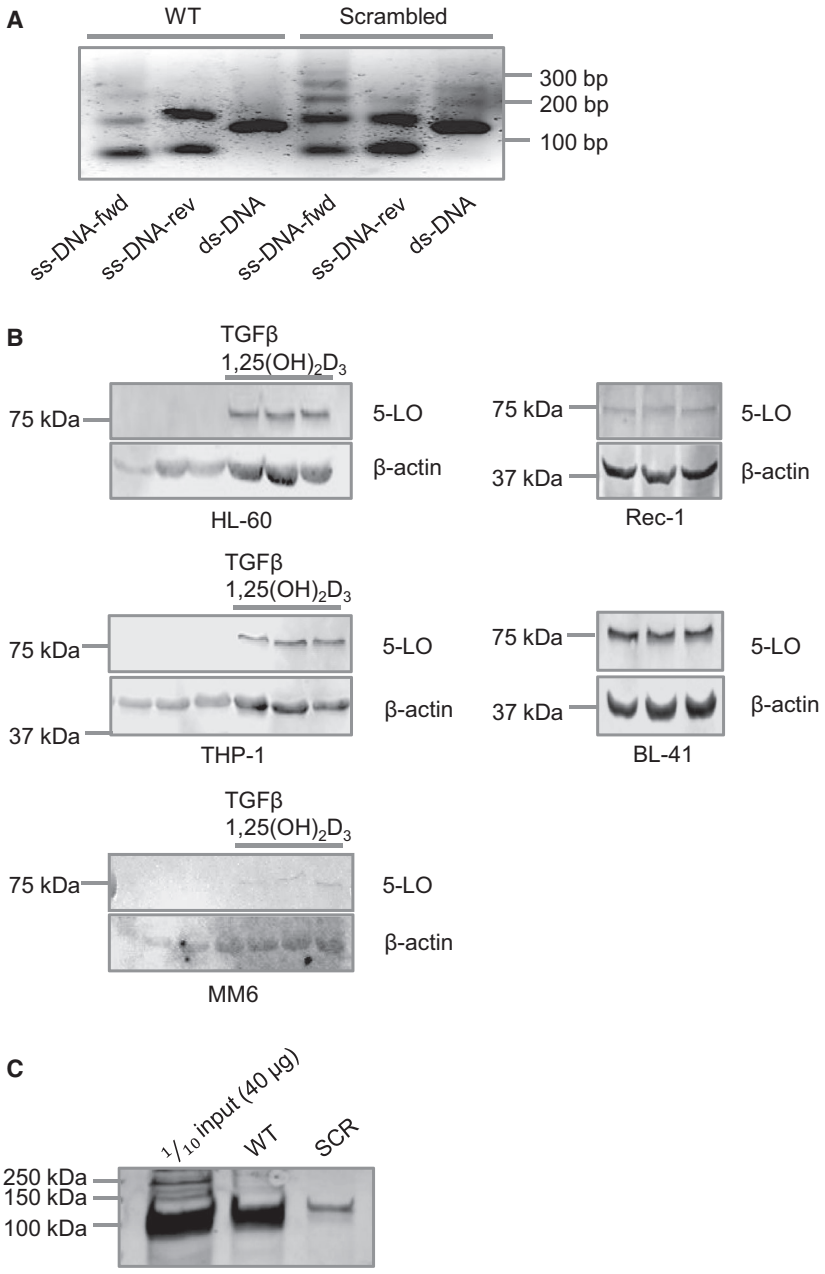

Fig. 3. Validation of the experimental set-up. (A) 3% Agarose gel electrophoresis to verify annealing of forward and reverse single-stranded sequences used in the DNA pulldowns. Sequences for ALOX 5 promoter oligonucleotides (WT) and SCR controls are given in Table S1. (B) 5-LO expression pattern in myeloid cell lines HL-60, THP1, MM6 and B-lymphocytic cell lines Rec-1 and BL-41. Myeloid cells were treated with TGFβ/1,25(OH)$_2$D$_3$ to induce differentiation and 5-LO protein expression. Samples from three consecutive cell passages were analysed in adjacent lanes. (C) Immunoblot from DNA pulldown with nuclear extract from the B-cell line Rec-1 to verify specific binding of the transcription factor Sp1 to the *ALOX5* promoter sequence (WT) as compared to SCR control. Four hundred microgram nuclear extract was used for each DNA fragment; the blotting membrane was probed with anti-Sp1 antibody (0.6 µg·mL^{-1}). The result from one out of three independent repetitions is shown.

biotinylated promoter DNA fragments in an ELISA. As DNA samples, we used fragments of the *ALOX5* promoter sequence that encompassed the 5-fold GC box, as this is the most likely part for building G-quadruplexes. The respective 46-mer oligonucleotides, of which the forward strands were 5′-biotinylated, were first subjected to annealing conditions in a buffer containing K^+ (100 mM) and subsequently coupled to streptavidin-coated 96-well plates. Oligonucleotides carrying mutations within the 5-fold GC box, and sequences from the *MYC* promoter known to form G-quadruplexes, were used as controls and treated analogously. Next, the DNA was probed with varying concentrations of the FLAG-tagged BG4 anti-G-quadruplex (concentration range 0.005–0.25 µg·mL^{-1}) and detection was carried out using an horseradish peroxidase (HRP)-coupled anti-FLAG secondary antibody and chromogenic substrate. As shown in Fig. 8A, the anti-G-quadruplex antibody binds with high affinity to the *MYC* and *ALOX5* sequences, but far less to the negative control (MUT) harbouring mutations in the GC box sequence. The binding

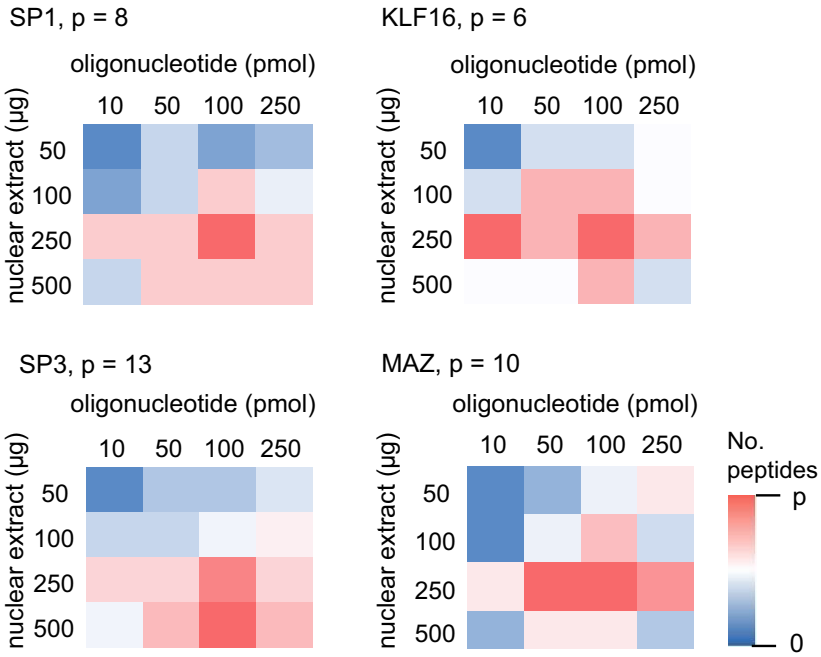

Fig. 4. Titration MS experiments to establish the standard amount of oligonucleotides and nuclear extract for each pulldown. Different amounts of *ALOX5* promoter oligonucleotide (10, 50, 100, 200 pmol; sequence see Table S1) were combined with varying amounts of nuclear extract (50, 100, 250, 500 µg) from the monocytic cell line MM6 and subjected to MS analysis. The number of peptides identified from the proteins SP1, KLF16, SP3 and MAZ (visualized by colour gradient) was plotted against the amounts of DNA oligonucleotide and nuclear extract in these 16 pulldowns. The colour gradient ranges from blue (little number of peptides found) to red (highest number of peptides found); p = maximum number of peptides found for the different proteins, respectively.

affinities for the *MYC* and the *ALOX5* sequences were comparable, indicating that the G-quadruplex formation properties of the *ALOX5* promoter are equivalent to a known example of a G-quadruplex regulated gene.

In order to confirm these results by distinct methods, we used spectroscopic approaches including CD- and UV–VIS spectroscopy. The latter was performed for analysing the interaction of the *ALOX5* promoter fragment and control DNA sequences with the agent Meso-5,10,15,20-Tetrakis-(N-methyl-4-pyridyl)porphine (TMPyP4). This cationic porphyrin is known to stabilize G-quadruplex DNA by stacking upon the tetrads, an interaction that can be detected by the degree of hypochromicity in absorbance titration experiments [51]. Subsequently, increasing concentrations of the DNA were added to a solution of TMPyP4 (5 µM) and absorption spectra in the range of 350–500 nm were recorded. As depicted in Fig. 8B a redshift of the intense peak at 422 nm (the Soret band of the porphyrin) could be observed with increasing amounts of DNA for all of the three oligonucleotides. Furthermore, an isosbestic point could be detected in a range of 431–435 nm in all cases. This indicates that, in principle, all of the sequences interact with TMPyP4. However, the decrease in absorbance for the Soret band was clearly sequence-dependent. For a negative control (CTR), a hypochromicity of 39.4% was observed, which correlates with reported interactions of TMPyP4 and duplex DNA [52]. In contrast, the absorption of the *MYC* and *ALOX5* WT sequences decreased to 49.1% and 54%, respectively, indicating the most effective stacking of TMPyP4 on the G-quadruplex structure for the *ALOX5* promoter sequence.

To corroborate the spectroscopic data received from the UV–VIS spectra, CD spectroscopy was used as a direct method for the analysis of G-quadruplex formation. The oligonucleotide sequences utilized corresponded to those used in ELISA and UV–VIS spectroscopy (Fig. 8A,B). As shown in Fig. 8C, the spectra obtained for the MYC and ALOX5 sequences revealed characteristic negative peaks at 241 and 242 nm and positive peaks at 262 and 266 nm, respectively. Both negative controls, containing either the mutant tandem GC box (MUT) or a control sequence (CTR), revealed positive peaks at around 280 nm each. The WT ALOX5 core promoter fragment additionally exhibited a peak at 293 nm, pointing to a topology that may originate from dimers forming parallel strand quartets with external loop residues, as found for certain telomere repeats [53].

Discussion

Here, we present a mass spectrometric identification of interaction partners of the *ALOX5* gene promoter, by which we add several as yet unrecognized proteins to the present knowledge of potential *ALOX5* gene regulators. We also confirm earlier reports on Sp-family proteins as specific binders of this genomic region.

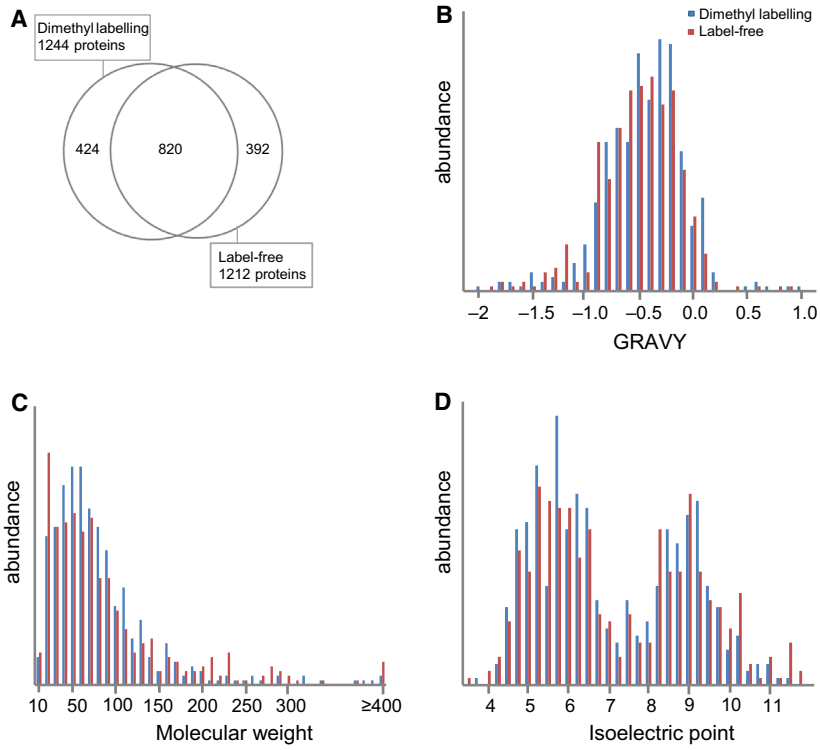

Fig. 5. Comparison of quantification strategies with samples from HL-60 DNA pulldowns. (A) Total number of identified proteins for dimethyl labelling and label-free quantification and overlap between both methods. (B–D) Properties of proteins identified exclusively in the different methods and respective abundances. Presented are (B) GRAVY-scores, (C) molecular weight and (D) isoelectric point in either blue (dimethyl labelling) or red (label-free).

Table 1. Comparison of mass spectrometry quantification methods. Total number of identified proteins and significant interactors for undifferentiated and differentiated HL-60 cells (HL-60/dHL-60) obtained by dimethyl labelling and label-free quantification.

Quantification method	Cell samples	Identified proteins	Significant interactors
Dimethyl labelling	HL-60	1244	5[a]
	dHL-60	1034	13[b]
Label-free	HL-60	1212	38[a]
	dHL-60	1121	20[b]

[a]Overlap: 4 proteins; [b]Overlap 6 proteins.

Previously, it has been demonstrated that the transcription factors Sp1 and Egr-1 bind to the tandem GC box of the proximal *ALOX5* promoter and that ectopic expression of these proteins induces reporter gene activity from *ALOX5* promoter constructs [21]. In a second study, it has been shown that Sp3 also binds to this sequence [54]. Our study provides confirmation that Sp1 and Sp3 are specific interactors of the *ALOX5* promoter, but we did not identify Egr-1 as specific binder in our analysis. Although peptides thereof could be found in two cellular conditions, it is most likely that this can be explained by the specific expression kinetics of this transcription factor. It has been shown for MM6 cells that Egr-1 was only present in these cells for 6 h after splitting the cell culture, in both untreated and TGFβ/calcitriol-treated cultures [55]. Our analysis, however, covers the proteins that are expressed at time points of steady-state *ALOX5* gene expression (72 h). Binding of Sp2 to the *ALOX5* promoter has as yet not been demonstrated. Due to its close relatedness to Sp1, it is plausible that this protein also plays a similar role in *ALOX5* gene control.

In our study, we included three myeloid cell lines of different basic maturation states and two different B-lymphocytic cell lines in order to analyse possible cell

Fig. 6. Volcano plots revealing significant interactors of the ALOX 5 promoter. DNA pulldowns with cell extracts from myeloid (A-C) and B-lymphocytic cell lines (D) were performed in triplicates and pulled-down proteins were quantified by label-free MS. Significant interactors were identified by *t*-test statistics, the results are displayed by volcano plots. The most relevant proteins (listed in Table 2) are given by their names, the others by their corresponding numbers from Table S2. In each graph, the ratio of label-free quantification intensities from pulldowns with WT vs. SCR DNA (log_2-transformed, *x*-axis) is plotted against and the *P* values of the *t*-test ($-log_{10}$-transformed, *y*-axis). The hyperbolic cut-off curves separate significant interactors (upper right area) from background. In detail, data are shown from pulldowns with (A) undifferentiated and differentiated HL-60 (dHL-60), (B) undifferentiated and differentiated THP-1 (dTHP-1), (C) undifferentiated and differentiated MM6 (dMM6) and (D) B-lymphocytic cell lines Rec-1 and BL41.

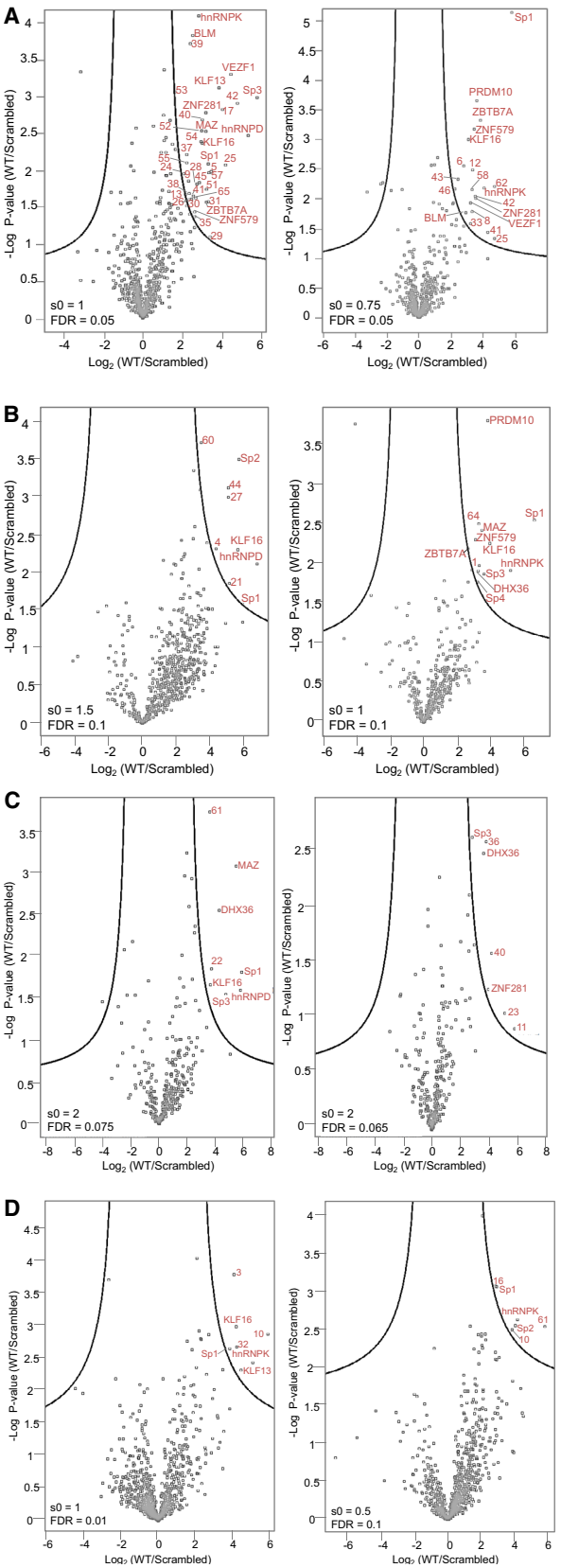
A
hnRNPK
BLM
39
VEZF1
KLF13
53
Sp3
42
ZNF281
17
40
MAZ
hnRNPD
52
54
KLF16
37
Sp1
25
55
24
28
5
49
45
57
38
51
41
65
26
30
31
ZBTB7A
35
ZNF579
29
s0 = 1
FDR = 0.05
-Log P-value (WT/Scrambled)
Log2 (WT/Scrambled)
Sp1
PRDM10
ZBTB7A
ZNF579
KLF16
6
12
43
58
62
46
hnRNPK
42
ZNF281
BLM
33
8
VEZF1
41
25
s0 = 0.75
FDR = 0.05
B
60
Sp2
44
27
4
KLF16
hnRNPD
21
Sp1
s0 = 1.5
FDR = 0.1
PRDM10
64
Sp1
MAZ
ZNF579
KLF16
ZBTB7A
1
hnRNPK
Sp3
DHX36
Sp4
s0 = 1
FDR = 0.1
C
61
MAZ
DHX36
22
Sp1
KLF16
Sp3
hnRNPD
s0 = 2
FDR = 0.075
Sp3
36
DHX36
40
ZNF281
23
11
s0 = 2
FDR = 0.065
D
3
KLF16
10
32
Sp1
hnRNPK
KLF13
s0 = 1
FDR = 0.01
16
Sp1
hnRNPK
61
Sp2
10
s0 = 0.5
FDR = 0.1

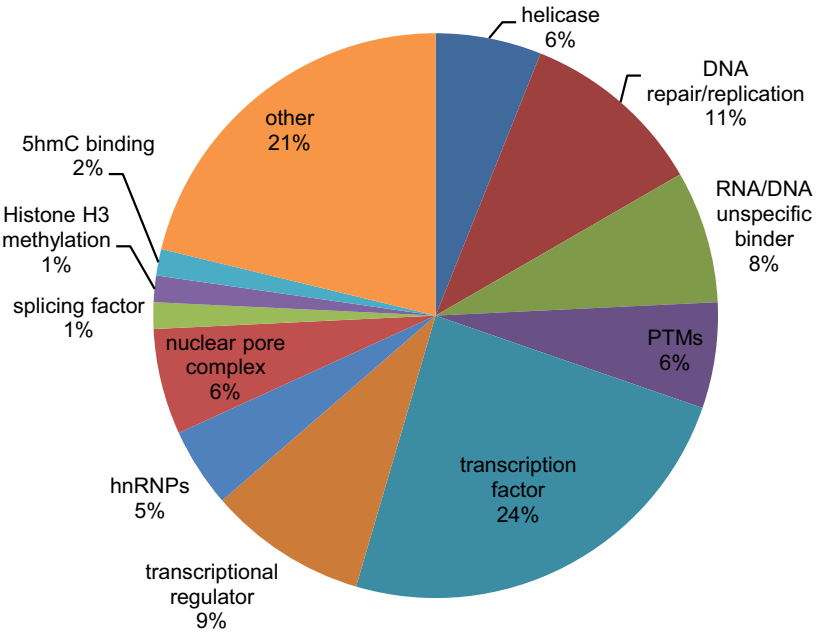

Fig. 7. Classification of proteins identified as significant *ALOX5* interactors. The 66 proteins that were identified as significant interactors of the *ALOX5* promoter in all experiments of this study (as listed in Table S2) were grouped according to their main biological function. The functional assignments were taken from the Uniprot database.

Table 2. Selection of significant *ALOX5* promoter-interacting proteins. Proteins identified as significant interactors in at least two cell sample types (d = differentiated) with known roles in gene regulation and number of unique peptides detected for these proteins.

Protein	HL-60	dHL-60	THP-1	dTHP-1	MM6	dMM6	Rec-1	BL-41	Unique peptides
BLM	x	x							(26 + 17)
DHX36				x	x	x			(3 + 2 + 1)
hnRNPD	x	x	x						(9 + 24 + 6)
hnRNPK	x	x		x			x	x	(46 + 45 + 16 + 65 + 68)
KLF13	x						x		(4 + 6)
KLF16	x	x	x	x	x		x		(2 + 1 + 8 + 1 + 5 + 6)
MAZ	x			x	x				(9 + 2 + 3)
PRDM10		x		x					(4 + 2)
Sp1	x	x	x	x	x		x	x	(7 + 5 + 9 + 10 + 5 + 17 + 18)
Sp2			x					x	(7 + 8)
Sp3	x			x	x	x			(8 + 11 + 7 + 1)
VEZF1	x	x							(9 + 10)
ZBTB7A	x	x		x					(6 + 22)
ZNF281	x	x				x			(14 + 29 + 2)
ZNF579	x	x		x					(3 + 5 + 8)

Fig. 8. *In vitro* evidence for the formation of G-quadruplex structures in the proximal human *ALOX5*-promoter sequence. (A) Indirect ELISA with anti-G-quadruplex antibody, clone BG4 and a 46-mer of the proximal *ALOX5* promoter sequence including the 5-fold tandem GC box (WT). As controls, a 22-mer of the *MYC* promoter sequence (MYC; positive control) and a mutated version of the WT sequence (MUT; negative control) were used (sequences see table). Biotinylated oligos were bound to streptavidin-coated 96-well plates and incubated with different concentrations of antibody BG4. After incubation with HRP-coupled secondary antibody and addition of substrate TMB, absorption was measured at 450 nm. Results are presented as means of $n = 3$, ±SD (B) Steady-state UV–VIS spectroscopy to verify the formation of G4-quadruplex structures. The quadruplex stabilizer TMPyP4 (5 μM) was incubated with increasing concentrations of the oligonucleotides WT, MYC and CTR (sequences see table), and absorbance was recorded in a range of 350–500 nm. This concentration range allowed for saturation of TMPyP4-DNA complex formation (no changes in the spectra after addition of 6, 8 and 10 μM oligonucleotides). Percentage of hypochromicity of the Soret band was calculated as stated in Materials and methods. All absorption spectra shown are averages of three experiments after correction for solvent. (C) CD spectra of oligonucleotides (5 μM) used in ELISA (A) and UV–VIS spectroscopy (B).

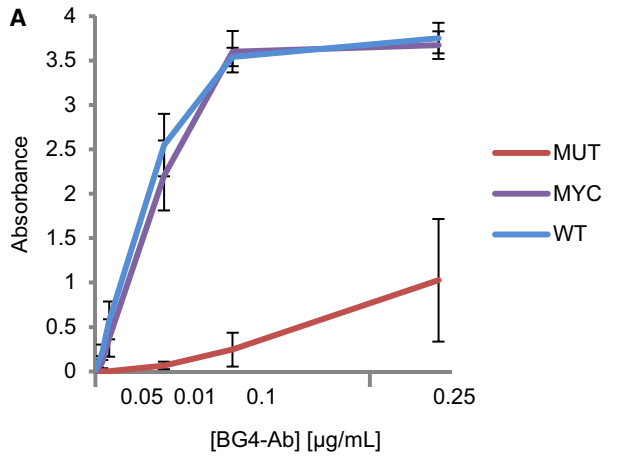

DNA	sequence
WT	[BIO]-GATCCTGCGG(GGGCGG)$_5$CAG
MYC	[BIO]-TGAGGGTGGGTAGGGTGGGTAA
MUT	[BIO]-GATCCTG(CGAATT)$_5$CAATTCAG

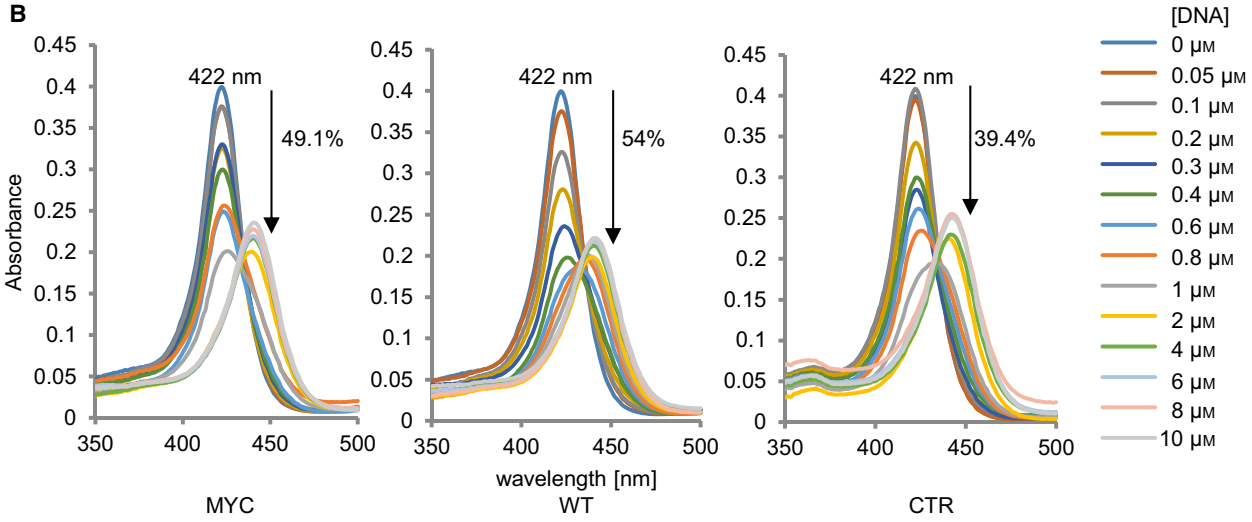

DNA	sequence	Shift Soret Band [nm]	Hypochromicity %
WT	[BIO]-GATCCTGCGG(GGGCGG)$_5$CAG	21	54
MYC	[BIO]-TGAGGGTGGGTAGGGTGGGTAA	18	49.1
CTR	GCTCGCCCCGCCCCGATCGAAT	20	39.4

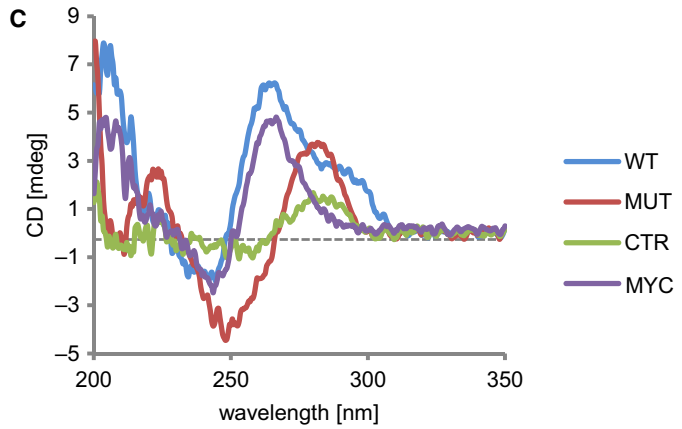

Table 3. Comparison of total protein numbers and of significant *ALOX5* promoter-interacting proteins from different cell samples. Presented are the number of proteins identified in total and the number of significant *ALOX5* promoter-interacting proteins for the different cell samples (d = differentiated). For the myeloid cell lines, the overlap between differentiated and undifferentiated cell states is given in the italic font.

Identified proteins	HL-60	dHL-60	THP-1	dTHP-1	MM6	dMM6	Rec-1	BL-41
Total	1212	1121	1559	743	606	544	2126	2215
Overlap undiff./diff.	*813*		*496*		*343*			
ALOX5 promotor interactors	38	20	9	12	8	7	7	6
Overlap interactors	*11*		*2*		*2*			

type-specific patterns of protein interactions with the *ALOX5* promoter. In the case of the three myeloid cell lines, we further analysed cell samples that were either treated with TGFβ/calcitriol or left untreated, to examine the influence of differentiation induction. However, in all cases, we identified a similar set of proteins, indicating that the differences in *ALOX5* gene expression known between these cell types and treatments might not be attributed to specific promoter occupation. Noticeable differences were present only for the number of identified specific interactors (a) in the different myeloid cell lines, showing a trend of decreasing numbers with increasing maturation state, and (b) less interactors in B cells as compared to the two less mature myeloid cell lines HL-60 and THP-1 (Table 3).

Only 4 out of 66 significant interactors were exclusively found in B cells, namely the mRNA binding protein CIRBP, the Src activator FAM120A, hnRNPU and the kinase regulatory protein THAP12. This set of proteins does not provide evidence for fundamental differences between B cells and myeloid cells regarding *ALOX5* promoter interactions.

For some of the proteins that we have identified in our analysis, evidence from ChIP-seq analysis of different cell types corroborates our findings. First, this is the case for the zinc finger protein MAZ, which we have identified as a specific interactor of the *ALOX5* promoter sequence in three sample types (undifferentiated HL-60, differentiated THP-1 and undifferentiated MM6). Indeed, ChIP-seq studies with the myelogenous leukaemia cell line K562 show MAZ binding to this genomic region. Second, binding of the transcription factor ZBTB7A, which we have identified as significant *ALOX5* interactor of the core promoter sequence in three myeloid cell samples, has also been mapped to this specific region. Further ChIP-seq data obtained from K562 cells demonstrate binding of the developmental transcription factor RUNX-1 to the proximal *ALOX5* promoter. We also identified RUNX-1 as specific binder, albeit only in pulldowns with nuclear extracts from TGFβ/calcitriol-treated HL-60 cells (Fig. S1).

For the other (putative) transcription factors that we have found in our study, it can as yet only be speculated about their significance in *ALOX5* gene regulation. The protein KLF13 has been shown to be a repressive transcription factor of the Sp/KLF family that competes with Sp1 for binding to GC boxes and plays a role in B- and T-cell development [56,57]. We have found specific binding of KLF13 to the *ALOX5* promoter with nuclear extracts from the B-cell line Rec-1 and from undifferentiated HL-60 cells, thus in myeloid cells that are still multipotent and more closely related to the common precursor of B cells and myeloid cells than THP-1 and MM6 cells. Therefore, this transcription factor might be relevant for the regulation of 5-LO expression in B cells and during the earlier stages of myeloid cell differentiation. KLF16, which we have identified as significant binder of the *ALOX5* promoter under six out of eight conditions (Table 2), is as yet functionally not well characterized. The latter is also the case for the potential histone methyltransferase PRDM10 and the (putative) transcription factors VEZF1 and ZNF579. Binding of KLF13, KLF16 ZNF579, VEZF1 and hnRNPK (see below) to the 5-LO promoter sequence has also been shown by ChIP-Seq analyses (Fig. S1). Very prominent signals in the 5-LO promoter were obtained for hnRNPK and ZNF579, which might explain their frequent hit in the MS analyses.

The transcription factor ZBTB7A (zinc finger and BTB domain-containing protein 7A) has been shown or predicted to repress transcription of genes involved in proliferation and differentiation by interacting with other factors, several of which have known or predicted binding sites near or at the *ALOX5* core promoter. These proteins include Sp1, SMAD4 as a central component of TGFβ signalling and the NFkB component RelA. In detail, it has been reported that ZBTB7A directly interacts with Sp1, thereby preventing its binding to DNA [58]. Further, ZBTB7A seems to recruit the corepressor component HDAC1 to SMAD4-DNA complexes [41] and it was further predicted by similarity analysis that ZBTB7A might

cooperate with RelA to regulate DNA accessibility for other transcription factors. For the developmental transcription factor ZNF281, it has been shown that its expression is induced by inflammatory stimuli and that the protein itself subsequently activates the expression of inflammatory genes [59], making *ALOX5* a plausible target of ZNF281 regulation. Intriguingly, many of the transcription factors that we have identified as significant *ALOX5* interactors have a role in developmental processes, supporting the observation that 5-LO possesses noncanonical functions in the regulation of cell proliferation and differentiation [60]. In order to shed light on the biological significance of these novel putative *ALOX5* regulators, *in cellulo* studies are needed to first assess their presence at the proximal *ALOX5* promoter in a cell type-specific and time-resolved manner and analyse their functional role in *ALOX5* gene regulation.

Five of the proteins that we have identified as specific interactors of the *ALOX5* promoter under at least two conditions (MAZ, BLM, DHX36, hnRNPD and hnRNPK) are associated with DNA G-quadruplexes. In this context, helicases BLM and DHX36 both resolve existing G4-DNA, whereas MAZ can exhibit dual function in their unwinding and stabilization [44,46,47,61,62]. The heterogeneous nuclear ribonucleoproteins are either known for unwinding telomere quadruplexes, as in the case of hnRNPD, or affecting *MYC* transcription in association with nucleolin by interacting with quadruplex sequences located in its promoter (both hnRNPD and hnRNPK) [48,49,63,64]. A further protein, YBX1, which we have detected as specific binder in pull-downs from differentiated HL-60 cells, has been proposed to be a G-quadruplex-interacting protein [65]. The identification of these proteins in our screening, combined with our *in vitro* evidence on G-quadruplex formation by the *ALOX5* proximal promoter sequence, led us to suggest that G-quadruplexes might play a role in *ALOX5* gene regulation. As yet, the notion that G-quadruplex structures are involved in transcriptional control is based on several lines of indirect evidence. First, it is known that G4-DNA targeting molecules (small molecules that stabilize G-quadruplexes or oligonucleotides that target G4 motifs) influence mRNA levels from genes that harbour such G4-DNA sequences in their promoters. Second, it has been observed that mutations in G-quadruplex-resolving helicases alter expression from genes that are rich in predicted G4-DNA structures. Thus, the detailed mechanism by which these DNA structures could regulate transcription is not yet fully elucidated. However, the knowledge of *ALOX5* as a putative G-quadruplex-regulated gene is of interest, as these structures provide a potential target for pharmacological intervention [66,67]. Therefore, our results provide the groundwork for further studies to evaluate the structural details of the quadruplex arrangement, its presence in the cellular context as well as interactions with proteins, and eventually the potential role of G-quadruplexes and associated protein complexes in 5-LO expression.

Materials and methods

Cell culture and preparation of nuclear extract

Monocytic cell lines HL-60, THP-1, MM6 and B-lymphocytes Rec-1, BL-41 were provided by Deutsche Sammlung von Mikroorganismen und Zellkulturen (DSMZ, Braunschweig, Germany). All cell lines except MM6 were cultured in RPMI 1640 + 10% FBS + 1% penicillin/streptomycin (all Thermo Fisher, Braunschweig, Germany) and supplemented with glutamine (2 mM; Thermo Fisher) at 5% CO_2, 37 °C. MM6 was cultured in RPMI 1640 supplemented with 10% FBS, 1% penicillin/streptomycin, nonessential amino acids, 10 $\mu g \cdot mL^{-1}$ insulin, 1 mM oxaloacetate and 1 mM sodium pyruvate in same conditions. Differentiation of monocytic cell lines was induced by the addition of 50 nM 1α,25-dihydroxyvitamin D_3 (Cayman Chemical, Ann Arbor, MI, USA) and 1 $ng \cdot mL^{-1}$ TGFβ (PeproTech, Hamburg, Germany) at 6% CO_2, 37 °C. Undifferentiated cells were seeded at 0.4×10^6 cells per mL, differentiated cells at 0.3×10^6 cells per mL and cells were harvested by centrifugation after 3 days of incubation. Cells were washed once with PBS. Nuclear extracts were prepared as described in Kloet *et al.* [31] and either stored at −80 °C until use or used freshly.

Annealing of oligonucleotides

Oligonucleotides of 120 bp were either synthesized by Sigma-Aldrich (Darmstadt, Germany) or IBA Life Sciences (Goettingen, Germany) as forward and reverse single-stranded DNA. All other oligonucleotides were purchased from Eurofins Genomics (Ebersberg, Germany) as single-stranded DNA. In all cases except for the control oligonucleotide used for UV spectroscopy, the 5'-end of the forward strand was biotinylated. For annealing of sequences, forward and complementary reverse strands were reconstituted in nuclease-free water and added in equal amounts to a buffer containing 10 mM Tris-HCl, pH 7.5, 50 mM NaCl, 1 mM EDTA to yield a final concentration of 10 $pmol \cdot \mu L^{-1}$. After incubation for 5 min at 95 °C, the solution was left to gradually cool down to room temperature. The successful formation of double-stranded DNA was monitored with 3% agarose gel electrophoresis.

Oligonucleotide sequences used for quadruplex experiments were annealed as single-strands in 10 mM Tris-HCl, pH 7.4, 100 mM KCl under the same conditions.

DNA pulldown

DNA pulldown and titration experiments were performed according to Hubner *et al.* [29] with modifications, as outlined in the following. After determining the protein concentration in the harvested nuclear extracts by Bradford assay, 300–400 µg lysate was incubated with 100 pmol dsDNA and 10 µg poly-dIdC in binding buffer [50 mM HEPES, pH 8.0, 150 mM NaCl, 0.1% NP-40, 1 mM DTT and complete protease inhibitor, EDTA-free (Roche, Mannheim, Germany) at 4 °C]. After 1.5 h, 100 µL streptavidin-coated magnetic beads (SeraMag™ SpeedBeads Blocked Streptavidin Particles; GE Healthcare Life Sciences, Freiburg, Germany), that had been washed in advance with conditioning buffer (10 mM Tris-HCl, pH 7.5, 1 mM EDTA, 2 M NaCl) and binding buffer, were added and incubation was continued for another half hour at 4 °C. After binding to the beads, the supernatant was discarded and pulled-down protein complexes were washed three times with binding buffer and wash buffer (100 mM ammonium bicarbonate, 150 mM NaCl) to remove any detergent present. After the first wash, fresh Eppendorf tubes (Eppendorf AG, Hamburg, Germany) were used to remove proteins that may have adsorbed to the tube wall. To establish the amounts of oligonucleotides and nuclear extract needed for the pulldowns, 10, 50, 100 and 250 pmol of DNA were incubated with 50, 100, 250 and 500 µg nuclear extract as described before.

Sample preparation for label-free MS quantification

For reduction/alkylation of the enriched proteins, beads were resuspended in 100 µL 25 mM ammonium bicarbonate and incubated with 9 mM dithioerythritol for 45 min at 57 °C and subsequently with 17 mM IAA for another 45 min at room temperature in the dark. The reaction was quenched by adding the same amounts of dithioerythritol once again for 15 min. Digestion was performed directly on the beads by adding 0.1 µg trypsin per sample at 37 °C for 15 h overnight. Digestion was continued with fresh trypsin (0.1 µg) for another hour the next day. Digestion was stopped by adding 1 µL of TFA. Afterwards, samples were purified via C18-spin columns (Thermo Fisher) according to the manufacturer's protocol.

Dimethyl labelling

Labelling reactions were carried out as described in Boersema *et al.* [37]. After binding of proteins to the beads and subsequent washing steps, beads were resuspended in 100 µL of 50 mM triethylammonium bicarbonate buffer, reduced and alkylated as described under 'sample preparation for label-free MS quantification' and digested overnight. After digestion, peptides were labelled by addition of 4 µL of either 4% CH_2O (light) or CD_2O (heavy). Subsequently, 4 µL of 0.6 M $NaBH_3CN$ was added to the each sample and incubation was continued for 1 h at room temperature with slight mixing. The reaction was quenched by adding 16 µL of 1% ammonia solution followed by 8 µL of formic acid afterwards. The corresponding light and heavy samples were combined, purified and dried by vacuum centrifugation for the following MS measurement. Dimethyl labelling pulldowns were performed twice with swatching of the respective labels.

LC-MS/MS

MS measurements were carried out on a Q-Exactive Plus mass spectrometer (Thermo Fisher Scientific), coupled to EASY-nLC1000. Samples were prepared as described above and dried using a vacuum centrifuge. For LC separation, samples were reconstituted in buffer A (0.1% formic acid in water), loaded onto a 50 cm Poroshell EC120 C18 column and run with a gradient from 3% to 95% solvent B (0.1% FA in acetonitrile) in buffer A over 150 min at a flow rate of 250 $nL \cdot min^{-1}$. MS1 scans were recorded in positive ion mode at a resolution of 70000, the following MS/MS spectra of the 10 most abundant signals at a resolution of 17500 (AGC 5×10^5, max. injection time 55 ms, isolation window 1.8 Da).

Data analysis

RAW data files were grouped according to their cell line and analysed with MAXQUANT software (version 1.6.0.1, https://www.maxquant.org) and in-built search engine Andromeda [68] with default settings. Oxidation (M), acetylation (N terminus) and deamidation (NQ) were set as variable, carbamidomethylation as fixed modification. For dimethyl labelling, multiplicity was set to 2 with the option of light (DimethLys0/DimethNter0) and heavy (DimethLys4/DimethNter4) label at the N terminus and lysines. For label-free identification, the match between runs option, and the label-free quantification and the iBAQ option were enabled. The identification of both proteins and peptides was accepted at a FDR of 0.01.

Further analysis was performed using PERSEUS (version 1.6.0.0, https://maxquant.net/perseus/) according to Hubner *et al.* [69]. Contaminants and reverse hits were filtered, and LFQ intensities were $\log_2$ transformed. Dimethyl labelled missing sample values were imputed (width 0.3, downshift 0.5) and significant interactors were determined by 'Significance B' test ($P \leq 0.05$). Proteins were visualized in scatter

plots. Label-free samples were grouped and filtered for three valid values in respective groups. Missing values were imputed with preset settings (width 0.3, downshift 1.8). The distribution of imputed values was checked with histograms. A two-sample *t*-test was applied, and significant interacting proteins were visualized by volcano plots. S0 and threshold values were adjusted separately for the different cell lines and states.

Immunoblotting

Protein samples for immunoblotting were generated from DNA pulldowns, which were performed as described above. Magnetic beads used for the pulldowns were washed three times with wash buffer B and were directly boiled in 20 µL Laemmli buffer for 5 min at 95 °C. After cooling, the whole 20 µL was loaded onto 10%-SDS polyacrylamide gels. Gel electrophoresis was carried out for 75 min at constant voltage of 75 V. Proteins were blotted on poly(vinylidene difluoride) membranes, blocked with Odyssey blocking buffer (Licor Biosciences, Bad Homburg, Germany) for 1 h at room temperature and incubated with the primary antibody (1 : 1000 dilution) overnight. Used antibodies comprise anti-Sp1 antibody (Thermo Fisher, PA5-29165), 5-LO in-house produced antibody 6A12, 5-LO antibody (Cell Signaling Technology, C49G1, Frankfurt, Germany). Protein of interest was detected with secondary antibody (1 : 10 000 dilution, IR-dye conjugated antibodies, Licor Biosciences) and quantified based on densitometry with correction for β-actin as loading control (Odyssey Imaging System; Licor Biosciences).

Indirect ELISA

Indirect ELISA was carried out with anti-DNA G-quadruplex structures antibody, clone BG4 (Merck, MABE917) as the primary antibody according to Lam *et al.* [70] with slight modifications. In detail, streptavidin high binding capacity coated 96-well plates (Thermo Scientific) were first washed three times with 200 µL wash buffer (25 mM Tris-HCl, pH 7.2, 150 mM NaCl, 0.1% BSA, 0.1% Tween 20) for 5 min. Plates were then coated with 50 nM oligonucleotides for 1 h at room temperature and subsequently washed three times afterwards with ELISA buffer (50 mM K_2HPO_4, pH 7.4, 100 mM KCl). Primary antibody was added in different concentrations (0, 0.005, 0.01, 0.05, 0.1, 0.25 $\mu g \cdot mL^{-1}$) and left to bind for another hour. Plates were washed with ELISA buffer supplemented with 0.1% Tween 20 and incubated with secondary antibody (HRP-anti-DDDDK-tag-ab; Abcam, Cambridge, UK, ab1238, dilution 1 : 100 000) for 1 h. After three more washes with ELISA buffer +0.1% Tween 20, 100 µL 3,3′,5,5′-Tetramethylbenzidine (TMB) substrate solution (Thermo Fisher) was added to the wells and stopped with 100 µL 0.18 M H_2SO_4. Absorbance was recorded at 450 nm with a Tecan plate reader (Tecan Spark; Tecan Trading AG, Männedorf, Switzerland).

UV–VIS spectroscopy

Absorption spectra were recorded on a Tecan plate reader in a range of 350–500 nm at room temperature. G-quadruplex stabilizing agent Meso-5,10,15,20-Tetrakis-(N-methyl-4-pyridyl)-porphin (TMPyp4) was purchased from Merck (No. 613560, Darmstadt, Germany). Stock solutions of TMPyP4 were prepared prior to the following experiments and kept in the dark. A serial dilution of annealed oligonucleotides was incubated for five minutes with 5 µM TMPyP4 in a total volume of 100 µL annealing buffer (see ′Annealing of oligonucleotides′). Final concentrations of all oligos were used at 0, 0.05, 0.1, 0.2, 0.3, 0.4, 0.6, 0.8, 1, 2, 3, 4, 6, 8 and 10 µM. Concentrations were chosen to not alter the shifting Soret band upon three subsequent additions of oligonucleotide anymore. All spectra shown are average spectra out of three measurements after correction for solvent effects.

The percentage of hypochromicity of the Soret band was calculated according to Wei *et al.* [71], where percentage hypochromicity = $((\varepsilon_{free} - \varepsilon_{bound})/\varepsilon_{free}) \times 100$. ε_{free} was calculated based on Lambert-Beer's law with $\varepsilon_{free} = A_{free}/C$, with a concentration C of free TMPyP4 of 5 µM. Absorbance was measured at the Soret maximum of TMPyP4 (422 nm). ε_{bound} can then be calculated with the equation $\varepsilon_{bound} = A_{bound}/C_{bound}$. A_{bound} in this case will be the absorbance of fully bound TMPyP4 at the Soret maximum, C_{bound} the concentration of bound TMPyP4 with $C_{bound} = C - C_{free}$ and $C_{free} = C(1-\alpha)$. The fraction of bound TMPyP4 α was calculated with $\alpha = (A_{free} - A)/(A_{free} - A_{bound})$, with the absorbance A_{free} and A_{bound} being the absorbances for free or fully bound TMPyP4 at the Soret maximum and A the absorbance at any given time point.

CD spectroscopy

CD spectra were recorded on a Jasco-810 spectrophotometer (Jasco, Pfungstadt, Germany) at room temperature (25 °C), using a quartz cell of 1 mm optical path length, an instrument scanning speed of 50 $nm \cdot min^{-1}$ and a response time of 1 s over a range of 200–350 nm. Depicted spectra are average spectra of five scans for each sample after correcting for solvent effects.

Oligonucleotides were diluted to a final concentration of 5 µM in annealing buffer as described (see ′Annealing of oligonucleotides′).

Acknowledgements

The authors acknowledge CECAD/CMMC Proteomics Core Facility, University of Cologne, Cologne 50931, Germany for MS measurements; Angelika Tintschl-Körbitzer for expert technical assistance and Dr. Ute Bahr for critical reading of the manuscript.

Conflict of interest

The authors declare no conflict of interest.

Author contributions

KS planned and performed experiments. MK and BS planned experiments. KS, DS, MK and BS analysed data and wrote the paper. BS conceived the project.

References

1 Rådmark O, Werz O, Steinhilber D & Samuelsson B (2015) 5-Lipoxygenase, a key enzyme for leukotriene biosynthesis in health and disease. *Biochim Biophys Acta* **1851**, 331–339.

2 Di Gennaro A & Haeggström JZ (2012) The leukotrienes: immune-modulating lipid mediators of disease. *Adv Immunol* **116**, 51–92.

3 Melstrom LG, Bentrem DJ, Salabat MR, Kennedy TJ, Ding X-Z, Strouch M, Rao SM, Witt RC, Ternent CA, Talamonti MS *et al.* (2008) Overexpression of 5-lipoxygenase in colon polyps and cancer and the effect of 5-LOX inhibitors *in vitro* and in a murine model. *Clin Cancer Res* **14**, 6525–6530.

4 Li N, Sood S, Wang S, Fang M, Wang P, Sun Z, Yang CS & Chen X (2005) Overexpression of 5-lipoxygenase and cyclooxygenase 2 in hamster and human oral cancer and chemopreventive effects of zileuton and celecoxib. *Clin Cancer Res* **11**, 2089–2096.

5 Hoque A, Lippman SM, Wu T-T, Xu Y, Liang ZD, Swisher S, Zhang H, Cao L, Ajani JA & Xu X-C (2005) Increased 5-lipoxygenase expression and induction of apoptosis by its inhibitors in esophageal cancer: a potential target for prevention. *Carcinogenesis* **26**, 785–791.

6 Steinhilber D & Hofmann B (2014) Recent advances in the search for novel 5-lipoxygenase inhibitors. *Basic Clin Pharmacol Toxicol* **114**, 70–77.

7 Wculek SK & Malanchi I (2015) Neutrophils support lung colonization of metastasis-initiating breast cancer cells. *Nature* **528**, 413–417.

8 Rådmark O, Werz O, Steinhilber D & Samuelsson B (2007) 5-Lipoxygenase: regulation of expression and enzyme activity. *Trends Biochem Sci* **32**, 332–341.

9 Busch S, Auth E, Scholl F, Huenecke S, Koehl U, Suess B & Steinhilber D (2015) 5-lipoxygenase is a direct target of miR-19a-3p and miR-125b-5p. *J Immunol* **194**, 1646–1653.

10 Tomimoto H, Shibata M, Ihara M, Akiguchi I, Ohtani R & Budka H (2002) A comparative study on the expression of cyclooxygenase and 5-lipoxygenase during cerebral ischemia in humans. *Acta Neuropathol* **104**, 601–607.

11 Brungs M, Radmark O, Samuelsson B & Steinhilber D (1994) On the induction of 5-lipoxygenase expression and activity in HL-60 cells: effects of vitamin D3, retinoic acid, DMSO and TGFβ. *Biochem Biophys Res Commun* **205**, 1572–1580.

12 Brungs M, Rådmark O, Samuelsson B & Steinhilber D (1995) Sequential induction of 5-lipoxygenase gene expression and activity in Mono Mac 6 cells by transforming growth factor beta and 1,25-dihydroxyvitamin D3. *Proc Natl Acad Sci USA* **92**, 107–111.

13 Jakobsson PJ, Steinhilber D, Odlander B, Rådmark O, Claesson HE & Samuelsson B (1992) On the expression and regulation of 5-lipoxygenase in human lymphocytes. *Proc Natl Acad Sci USA* **89**, 3521–3525.

14 Werz O & Steinhilber D (1996) Selenium-dependent peroxidases suppress 5-lipoxygenase activity in B-lymphocytes and immature myeloid cells: the presence of peroxidase-insensitive 5-lipoxygenase activity in differentiated myeloid cells. *Eur J Biochem* **242**, 90–97.

15 Ahmad K, Scholz B, Capelo R, Schweighöfer I, Kahnt AS, Marschalek R & Steinhilber D (2015) AF4 and AF4-MLL mediate transcriptional elongation of 5-lipoxygenase mRNA by 1, 25-dihydroxyvitamin D3. *Oncotarget* **6**, 25784–25800.

16 Saul MJ, Groher F, Hegewald AB, Müller-McNicoll M, Marschalek R, Suess B & Steinhilber D (2017) TGFβ/SMAD signalling modulates MLL and MLL-AF4 mediated 5-lipoxygenase promoter activation. *Prostaglandins Other Lipid Mediat* **133**, 60–67.

17 Härle D, Rådmark O, Samuelsson B & Steinhilber D (1998) Calcitriol and transforming growth factor-β upregulate 5-lipoxygenase mRNA expression by increasing gene transcription and mRNA maturation. *Eur J Biochem* **254**, 275–281.

18 Stoffers KL, Sorg BL, Seuter S, Rau O, Rådmark O & Steinhilber D (2010) Calcitriol upregulates open chromatin and elongation markers at functional vitamin D response elements in the distal part of the 5-lipoxygenase gene. *J Mol Biol* **395**, 884–896.

19 Uhl J, Klan N, Rose M, Entian K-D, Werz O & Steinhilber D (2002) The 5-lipoxygenase promoter is regulated by DNA methylation. *J Biol Chem* **277**, 4374–4379.

20 Hoshiko S, Rådmark O & Samuelsson B (1990) Characterization of the human 5-lipoxygenase gene promoter. *Proc Natl Acad Sci USA* **87**, 9073–9077.

21 Silverman ES, Du J, De Sanctis GT, Rådmark O, Samuelsson B, Drazen JM & Collins T (1998) Egr-1 and Sp1 interact functionally with the 5-lipoxygenase promoter and its naturally occurring mutants. *Am J Respir Cell Mol Biol* **19**, 316–323.

22 In KH, Asano K, Beier D, Grobholz J, Finn PW, Silverman EK, Silverman ES, Collins T, Fischer AR, Keith TP *et al.* (1997) Naturally occurring mutations in the human 5-lipoxygenase gene promoter that modify

transcription factor binding and reporter gene transcription. *J Clin Invest* **99**, 1130–1137.
23 Drazen JM, Yandava CN, Dubé L, Szczerback N, Hippensteel R, Pillari A, Israel E, Schork N, Silverman ES, Katz DA *et al.* (1999) Pharmacogenetic association between ALOX5 promoter genotype and the response to anti-asthma treatment. *Nat Genet* **22**, 168–170.
24 Aebersold R & Mann M (2003) Mass spectrometry-based proteomics. *Nature* **422**, 198.
25 Gstaiger M & Aebersold R (2009) Applying mass spectrometry-based proteomics to genetics, genomics and network biology. *Nat Rev Genet* **10**, 617–627.
26 Megger DA, Bracht T, Meyer HE & Sitek B (2013) Label-free quantification in clinical proteomics. *Biochim Biophys Acta* **1834**, 1581–1590.
27 Vermeulen M, Hubner NC & Mann M (2008) High confidence determination of specific protein–protein interactions using quantitative mass spectrometry. *Curr Opin Biotechnol* **19**, 331–337.
28 Altelaar AFM, Munoz J & Heck AJR (2013) Next-generation proteomics: towards an integrative view of proteome dynamics. *Nat Rev Genet* **14**, 35–48.
29 Hubner NC, Nguyen LN, Hornig NC & Stunnenberg HG (2015) A quantitative proteomics tool to identify DNA–protein interactions in primary cells or blood. *J Proteome Res* **14**, 1315–1329.
30 Keilhauer EC, Hein MY & Mann M (2015) Accurate protein complex retrieval by affinity enrichment mass spectrometry (AE-MS) rather than affinity purification mass spectrometry (AP-MS). *Mol Cell Proteomics* **14**, 120–135.
31 Kloet SL, Baymaz H, Makowski M, Groenewold V, Jansen PW, Berendsen M, Niazi H, Kops GJ & Vermeulen M (2015) Towards elucidating the stability, dynamics and architecture of the nucleosome remodeling and deacetylase complex by using quantitative interaction proteomics. *FEBS J* **282**, 1774–1785.
32 Smits AH, Jansen PWTC, Poser I, Hyman AA & Vermeulen M (2013) Stoichiometry of chromatin-associated protein complexes revealed by label-free quantitative mass spectrometry-based proteomics. *Nucleic Acids Res* **41**, e28–e28.
33 Murat P & Balasubramanian S (2014) Existence and consequences of G-quadruplex structures in DNA. *Curr Opin Genet Dev* **25**, 22–29.
34 Collins SJ (1987) The HL-60 promyelocytic leukemia cell line: proliferation, differentiation, and cellular oncogene expression. *Blood* **70**, 1233–1244.
35 Karimi K, Gemmill TR & Lennartz MR (1999) Protein kinase C and a calcium-independent phospholipase are required for IgG-mediated phagocytosis by Mono-Mac-6 cells. *J Leukoc Biol* **65**, 854–862.
36 Wöbke TK, von Knethen A, Steinhilber D & Sorg BL (2013) CD69 Is a TGF-β/1α,25-dihydroxyvitamin D3 target gene in monocytes. *PLoS One* **8**, e64635.
37 Boersema PJ, Raijmakers R, Lemeer S, Mohammed S & Heck AJR (2009) Multiplex peptide stable isotope dimethyl labeling for quantitative proteomics. *Nat Protoc* **4**, 484–494.
38 Song J, Ugai H, Kanazawa I, Sun K & Yokoyama KK (2001) Independent repression of a GC-rich housekeeping gene by Sp1 and MAZ involves the same cis-elements. *J Biol Chem* **276**, 19897–19904.
39 Bossone SA, Asselin C, Patel AJ & Marcu KB (1992) MAZ, a zinc finger protein, binds to c-MYC and C2 gene sequences regulating transcriptional initiation and termination. *Proc Natl Acad Sci USA* **89**, 7452–7456.
40 Jeon B-N, Yoo J-Y, Choi W-I, Lee C-E, Yoon H-G & Hur M-W (2008) Proto-oncogene FBI-1 (Pokemon/ZBTB7A) represses transcription of the tumor suppressor Rb gene via binding competition with Sp1 and recruitment of co-repressors. *J Biol Chem* **283**, 33199–33210.
41 Yang Y, Cui J, Xue F, Zhang C, Mei Z, Wang Y, Bi M, Shan D, Meredith A, Li H *et al.* (2015) Pokemon (FBI-1) interacts with Smad4 to repress TGF-β-induced transcriptional responses. *Biochim Biophys Acta* **1849**, 270–281.
42 Hahn S & Hermeking H (2014) ZNF281/ZBP-99: a new player in epithelial–mesenchymal transition, stemness, and cancer. *J Mol Med* **92**, 571–581.
43 Law DJ, Du M, Law GL & Merchant JL (1999) ZBP-99 defines a conserved family of transcription factors and regulates ornithine decarboxylase gene expression. *Biochem Biophys Res Commun* **262**, 113–120.
44 Palumbo SL, Memmott RM, Uribe DJ, Krotova-Khan Y, Hurley LH & Ebbinghaus SW (2008) A novel G-quadruplex-forming GGA repeat region in the c-myb promoter is a critical regulator of promoter activity. *Nucleic Acids Res* **36**, 1755–1769.
45 Ponton A, Thirion J-P & Siroie P (1997) Repression of the 5-lipoxygenase gene by c-myb overexpression in differentiated HL-60 cells. *Prostaglandins* **53**, 49–58.
46 Sun H, Karow JK, Hickson ID & Maizels N (1998) The Bloom's syndrome helicase unwinds G4 DNA. *J Biol Chem* **273**, 27587–27592.
47 Vaughn JP, Creacy SD, Routh ED, Joyner-Butt C, Jenkins GS, Pauli S, Nagamine Y & Akman SA (2005) The DEXH protein product of the DHX36 gene is the major source of tetramolecular quadruplex G4-DNA resolving activity in HeLa cell lysates. *J Biol Chem* **280**, 38117–38120.
48 Enokizono Y, Konishi Y, Nagata K, Ouhashi K, Uesugi S, Ishikawa F & Katahira M (2005) Structure of hnRNP D complexed with single-stranded telomere DNA and unfolding of the quadruplex by

heterogeneous nuclear ribonucleoprotein D. *J Biol Chem* **280**, 18862–18870.
49 Uribe DJ, Guo K, Shin Y-J & Sun D (2011) Heterogeneous nuclear ribonucleoprotein K and nucleolin as transcriptional activators of the vascular endothelial growth factor promoter through interaction with secondary DNA structures. *Biochemistry* **50**, 3796–3806.
50 Biffi G, Tannahill D, McCafferty J & Balasubramanian S (2013) Quantitative visualization of DNA G-quadruplex structures in human cells. *Nat Chem* **5**, 182–186.
51 Haq I, Trent JO, Chowdhry BZ & Jenkins TC (1999) Intercalative G-tetraplex stabilization of telomeric DNA by a cationic porphyrin1. *J Am Chem Soc* **121**, 1768–1779.
52 Arora A & Maiti S (2008) Effect of loop orientation on quadruplex−TMPyP4 interaction. *J Phys Chem B* **112**, 8151–8159.
53 Rujan IN, Meleney JC & Bolton PH (2005) Vertebrate telomere repeat DNAs favor external loop propeller quadruplex structures in the presence of high concentrations of potassium. *Nucleic Acids Res* **33**, 2022–2031.
54 Schnur N, Seuter S, Katryniok C, Rådmark O & Steinhilber D (2007) The histone deacetylase inhibitor trichostatin A mediates upregulation of 5-lipoxygenase promoter activity by recruitment of Sp1 to distinct GC-boxes. *Biochim Biophys Acta* **1771**, 1271–1282.
55 Dishart D, Schnur N, Klan N, Werz O, Steinhilber D, Samuelsson B & Rådmark O (2005) GC-rich sequences in the 5-lipoxygenase gene promoter are required for expression in Mono Mac 6 cells, characterization of a novel Sp1 binding site. *Biochim Biophys Acta* **1738**, 37–47.
56 Kaczynski J, Zhang J-S, Ellenrieder V, Conley A, Duenes T, Kester H, van der Burg B & Urrutia R (2001) The Sp1-like protein BTEB3 inhibits transcription via the basic transcription element box by interacting with mSin3A and HDAC-1 co-repressors and competing with Sp1. *J Biol Chem* **276**, 36749–36756.
57 Outram SV, Gordon AR, Hager-Theodorides AL, Metcalfe J, Crompton T & Kemp P (2008) KLF13 influences multiple stages of both B and T cell development. *Cell Cycle* **7**, 2047–2055.
58 Lee D-K, Suh D, Edenberg HJ & Hur M-W (2002) POZ domain transcription factor, FBI-1, represses transcription of ADH5/FDH by interacting with the zinc finger and interfering with DNA binding activity of Sp1. *J Biol Chem* **277**, 26761–26768.
59 Pierdomenico M, Palone F, Cesi V, Vitali R, Mancuso AB, Cucchiara S, Oliva S, Aloi M & Stronati L (2018) Transcription factor ZNF281: a novel player in intestinal inflammation and fibrosis. *Front Immunol* **9**, 2907.
60 Häfner A-K, Kahnt AS & Steinhilber D (2019) Beyond leukotriene formation—The noncanonical functions of 5-lipoxygenase. *Prostaglandins Other Lipid Mediat* **142**, 24–32.
61 Membrino A, Cogoi S, Pedersen EB & Xodo LE (2011) G4-DNA formation in the HRAS promoter and rational design of decoy oligonucleotides for cancer therapy. *PLOS One* **6**, e24421.
62 Cogoi S, Paramasivam M, Membrino A, Yokoyama KK & Xodo LE (2010) The KRAS promoter responds to Myc-associated zinc finger and poly(ADP-ribose) polymerase 1 proteins, which recognize a critical quadruplex-forming GA-element. *J Biol Chem* **285**, 22003–22016.
63 Brys A & Maizels N (1994) LR1 regulates c-myc transcription in B-cell lymphomas. *Proc Natl Acad Sci USA* **91**, 4915–4919.
64 González V, Guo K, Hurley L & Sun D (2009) Identification and characterization of nucleolin as a c-myc G-quadruplex-binding protein. *J Biol Chem* **284**, 23622–23635.
65 Byrd AK, Zybailov BL, Maddukuri L, Gao J, Marecki JC, Jaiswal M, Bell MR, Griffin WC, Reed MR, Chib S *et al.* (2016) Evidence that G-quadruplex DNA accumulates in the cytoplasm and participates in stress granule assembly in response to oxidative stress. *J Biol Chem* **291**, 18041–18057.
66 Balasubramanian S & Neidle S (2009) G-quadruplex nucleic acids as therapeutic targets. *Curr Opin Chem Biol* **13**, 345–353.
67 Neidle S (2016) Quadruplex nucleic acids as novel therapeutic targets. *J Med Chem* **59**, 5987–6011.
68 Cox J & Mann M (2008) MaxQuant enables high peptide identification rates, individualized p.p.b.-range mass accuracies and proteome-wide protein quantification. *Nat Biotechnol* **26**, 1367–1372.
69 Hubner NC, Bird AW, Cox J, Splettstoesser B, Bandilla P, Poser I, Hyman A & Mann M (2010) Quantitative proteomics combined with BAC TransgeneOmics reveals *in vivo* protein interactions. *J Cell Biol* **189**, 739–754.
70 Lam EYN, Beraldi D, Tannahill D & Balasubramanian S (2013) G-quadruplex structures are stable and detectable in human genomic DNA. *Nat Commun* **4**, 1796.
71 Wei C, Jia G, Yuan J, Feng Z & Li C (2006) A spectroscopic study on the interactions of porphyrin with G-quadruplex DNAs. *Biochemistry* **45**, 6681–6691.

Supporting information

Additional supporting information may be found online in the Supporting Information section at the end of the article.

Fig. S1. ChIP-seq data showing binding of various transcription factors within the ALOX 5 gene.

Table S1. 120-mer single-stranded forward and reverse oligonucleotide sequences used for pulldown experiments.

Table S2. Overview of all significant ALOX5 interacting proteins identified from DNA pulldowns with myeloid and B-lymphocytic cell lines.